Available online at www.sciencedirect.com
SCIENCE DIRECT®
International Journal of Heat and Mass Transfer 47 (2004) 2233–2239
International Journal of HEAT and MASS TRANSFER
www.elsevier.com/locate/ijhmt

Conjugate of natural convection and conduction in a complicated enclosure

Shao-Feng Dong, Yin-Tang Li *

Environmental Center, Xi'an jiaotong University, Xi'an, Shannxi 710049, PR China

Received 29 August 2003; received in revised form 15 November 2003

Abstract

Natural convection of fluid and solid conjugate problem inside a complex cavity is studied by using vorticity–stream function method. The influences of material character, geometrical shape and Rayleigh number on the heat transfer in overall concerned region have been investigated. The followings can be concluded under steady state: The flow and heat transfer increase with the increase of the thermal conductivity in solid region; Both geometric shape and Rayleigh number affect the overall flow and heat transfer greatly.

Keywords: Natural convection; Conjugate between convection and conduction; Numerical simulation

1. Introduction

The phenomenon of two-dimension natural convection in an enclosure is widely used in engineering such as solar energy collector, heat preservation of thermal transport circuits, cooling of electrical units, etc. It has been intensively researched last century. Natural convections in cavity of various shape and many kinds of boundary conditions have been simulated [1–3]. Convection flow in partially open enclosure has been investigated [4]. Natural convection inside the channel between the flat-plate cover and sine-wave absorber of a cross-corrugate solar air heater has been discussed by Gao et al. [5] in 1999. Their model is very similar to the solar energy collector. Liu and Tao [6] have studied the natural convection around a vertical channel in a rectangular enclosure in 1996. In their calculation the influence of vertical channel walls to the flow is taken into account, but the channel walls are iso-thermal. The main aims of such simulations or experiments are to find the relations between dimensionless parameters and resulted fluid and heat transfer characteristics. But many studies have been done before simplify the models by considering the adiabatic boundary as a wall of infinite small thickness or wall with zero conductivity, this is ideal adiabatic boundary condition. Some simulations modeling a solid region in flow area neglect the heat transfer in the solid regions. These assumptions simplify problems and make them ease to study, but do not apply in the engineering practice and experiments very well.

Experiment about the natural convection in a cavity where a heated cylinder located in the center has been conducted by Cesini et al. [7]. In their experiment the upper wall is bounded by plexiglas whose thermal properties are known and there is a certain heat flux at its outside. In their experiment conduction of the plexiglas is taken into consideration. A numerical study of convection heat transfer for air from two vertically separated horizontal heated cylinders confined to a rectangular enclosure has been conducted [8], where the vertical walls have finite conductivity and the heat conduction has been taken into consideration. In this paper we also take the interactions between conduction in solid wall and convection of fluid region into account and simulate the heat transfer in a complicated enclosure with vorticity–stream function method.

As shown in Fig. 1, a horizontal high temperature (T_h) cylinder (e) of diameter D is enclosed by a cavity of rectangular cross-section ($H \times W$), both vertical side walls noted as (a) and (b) in Fig. 1 of this cross-section

* Corresponding author. Tel./fax: +86-29-82667940.
E-mail address: ytli@mail.xjtu.edu.cn (Y.-T. Li).

0017-9310/$ - see front matter © 2003 Elsevier Ltd. All rights reserved.
doi:10.1016/j.ijheatmasstransfer.2003.11.018

Nomenclature

A	aspect ratio H/W
B	relative diameter of horizontal cylinder, ratio D/W
C	relative thickness of solid region, ratio h/W
D	diameter of the high temperature circle (m)
g	gravitational acceleration ($m\,s^{-2}$)
h	thickness of solid wall (m)
H	height of constant low temperature wall (m)
k	thermal conductivity ratio $k = k_s/k_f$
k_f	thermal conductivity of fluid ($W\,m^{-1}\,K^{-1}$)
k_s	thermal conductivity of solid wall ($W\,m^{-1}\,K^{-1}$)
Nu	local Nusselt number on the high temperature circle, Eq. (10)
Nu_{mean}	overall mean Nusselt number of the high temperature circle, cf. Eq. (11)
Ra	Rayleigh number
T_h	hot wall temperature (K)
T_c	cold wall temperature (K)
T	dimensional temperature (K)
t	dimensional time (s)
u, v	velocity components in x, y directions ($m\,s^{-1}$)
U, V	dimensionless velocity components in X, Y directions
W	length of adiabatic boundary (m)
x, y	dimensional Cartesian coordinates (m)
X, Y	dimensionless Cartesian coordinates
X_c, Y_c	the center coordinates of the high temperature circle
T^*	dimensionless temperature
T^*_{ns}	dimensionless grid temperature nearest to the interface in the solid region
T^*_{nf}	dimensionless grid temperature nearest to interface in the flow field

Greek symbols

α_f	thermal diffusivity of the fluid ($m^2 s^{-1}$)
a_s	thermal diffusivity of the solid ($m^2 s^{-1}$)
β	coefficient of thermal expansion of the fluid (K^{-1})
v	kinematic viscosity of the fluid ($m^2\,s^{-1}$)
ρ	density of the fluid ($kg\,m^{-3}$)
φ	stream function
ω	vorticity

Subscripts

c	cold wall
f	fluid
h	hot wall
nf	nearest nodes in fluid field
ns	nearest nodes in solid region
s	solid wall

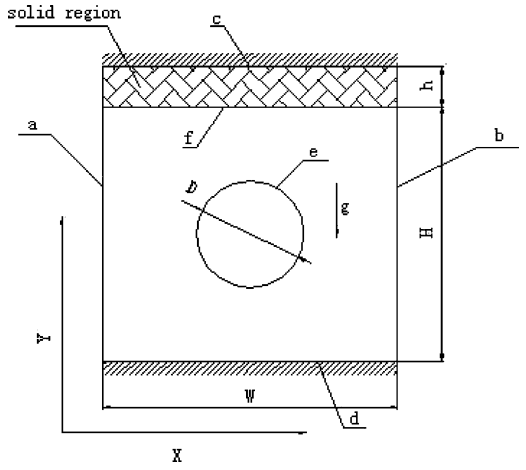

Fig. 1. Model.

are isothermal, the temperature is T_c. The upper horizontal boundary (f) of the rectangular is surrounded by solid material with constant thermal conductivity k_s and thermal diffusivity a_s. The upper of this solid region horizontal boundary symbolized by 'c' is considered as adiabatic. The lower horizontal boundary (d) of this cavity is supposed as ideal adiabatic boundary with infinite small wall thickness and zero thermal conductivity. All dimensions and boundaries of our model are noted in Fig. 1.

In this paper we changed the dynamic parameter mainly Ra and thermal characteristics of solid region material to simulate the heat transfer under different conditions. We also varied the geometric shapes of our model such as aspect ratio, relative thickness of solid region, relative diameter of the high temperature cylinder to discuss their influence on the characteristics of relevant resulting flow and heat transfer. We defined dimensionless parameter Nu_{mean} to measure and compare the flow and heat transfer intensity. Details of Nu and Nu_{mean} are described clearly in part 3. In order to comparison, we also defined some geometric parameters as

$$A = \frac{H}{W}, \quad B = \frac{D}{W}, \quad C = \frac{h}{W}$$

2. Governing equations and numerical method

2.1. Governing equations

By introducing the Boussinesq approximation and effective pressure into two-dimension natural convection, including the temperature equations, the whole equations of our model can be written as

$$\frac{\partial}{\partial x}\left(\omega\frac{\partial\varphi}{\partial y}\right)-\frac{\partial}{\partial y}\left(\omega\frac{\partial\varphi}{\partial x}\right)=v\left(\frac{\partial^2\omega}{\partial x^2}+\frac{\partial^2\omega}{\partial y^2}\right)-g\beta\left(\frac{\partial T_{\mathrm{f}}}{\partial x}\right) \tag{1}$$

$$\frac{\partial^2\varphi}{\partial x^2}+\frac{\partial^2\varphi}{\partial y^2}=\omega \tag{2}$$

$$\frac{\partial T_{\mathrm{f}}}{\partial t}+\frac{\partial}{\partial x}\left(T_{\mathrm{f}}\frac{\partial\varphi}{\partial y}\right)-\frac{\partial}{\partial y}\left(T_{\mathrm{f}}\frac{\partial\varphi}{\partial x}\right)=a_{\mathrm{f}}\left(\frac{\partial^2T_{\mathrm{f}}}{\partial x^2}+\frac{\partial^2T_{\mathrm{f}}}{\partial y^2}\right) \tag{3}$$

$$\frac{\partial T_{\mathrm{s}}}{\partial t}=a_{\mathrm{s}}\left(\frac{\partial^2T_{\mathrm{s}}}{\partial x^2}+\frac{\partial^2T_{\mathrm{s}}}{\partial y^2}\right)\quad\text{(in solid region)} \tag{4}$$

Here in our equations from (1)–(4) the internal relations of these variables are

$$u=\frac{\partial\varphi}{\partial y},\quad v=-\frac{\partial\varphi}{\partial x},\quad \omega=\frac{\partial u}{\partial y}-\frac{\partial v}{\partial x}$$

It can be seen that the definition of vorticity here is opposite to conventional definition in fluid dynamics. We take the width of the cavity (adiabatic boundary scale) W as reference length and introduce the following dimensionless variables

$$X=\frac{x}{W},\quad Y=\frac{y}{W},\quad T^*=\frac{T-T_{\mathrm{c}}}{T_{\mathrm{h}}-T_{\mathrm{c}}},\quad \overline{\omega}=\frac{\omega W^2}{v},\quad \overline{\varphi}=\frac{\varphi}{v}$$

$$Ra=g\beta\Delta TW^3/\alpha_{\mathrm{f}}v$$

Eqs. from (1)–(4) are changed into the following:

$$\frac{\partial}{\partial X}\left(\overline{\omega}\frac{\partial\overline{\varphi}}{\partial Y}\right)-\frac{\partial}{\partial Y}\left(\overline{\omega}\frac{\partial\overline{\varphi}}{\partial X}\right)=\left(\frac{\partial^2\overline{\omega}}{\partial X^2}+\frac{\partial^2\overline{\omega}}{\partial Y^2}\right)-\frac{Ra}{P_r}\left(\frac{\partial T^*}{\partial X}\right) \tag{5}$$

$$\left(\frac{\partial^2\overline{\varphi}}{\partial X^2}+\frac{\partial^2\overline{\varphi}}{\partial Y^2}\right)=\overline{\omega} \tag{6}$$

$$\frac{\partial T_{\mathrm{f}}^*}{\partial t}+\frac{\partial}{\partial X}\left(T_{\mathrm{f}}^*\frac{\partial\overline{\varphi}}{\partial Y}\right)-\frac{\partial}{\partial Y}\left(T_{\mathrm{f}}^*\frac{\partial\overline{\varphi}}{\partial X}\right)=\frac{1}{P_r}\left(\frac{\partial^2T_{\mathrm{f}}^*}{\partial X^2}+\frac{\partial^2T_{\mathrm{f}}^*}{\partial Y^2}\right)\quad(0\leqslant Y\leqslant A) \tag{7}$$

$$\frac{\partial T_{\mathrm{s}}^*}{\partial t}=\frac{1}{W^2}\times a_{\mathrm{s}}\times\left(\frac{\partial^2T_{\mathrm{s}}^*}{\partial X^2}+\frac{\partial^2T_{\mathrm{s}}^*}{\partial Y^2}\right)\quad(A\leqslant Y\leqslant A+C). \tag{8}$$

In convenient to comparison we defined

$$k=k_{\mathrm{s}}/k_{\mathrm{f}}$$

For steady state two-dimension natural flow, Eq. (8) is a standard thermal diffusive equation without source or sink. Then we can deduce the flow and heat transfer are not affected by a_{s} at all.

2.2. Boundary condition

2.2.1. Vorticity

We use Wood formula [9] to calculate the vorticity on boundary

$$\overline{\omega_1}=\frac{3(\overline{\varphi_2}-\overline{\varphi_1})}{\delta Y^2}-\frac{\overline{\omega_2}}{2}+\mathrm{O}(\delta Y^2)$$

(Boundary (a), (b), (f) and (d) shown in Fig. 1)

in which subscript 1 represents nodes on boundary and 2 represents the nearest internal nodes neighbor to this boundary.

2.2.2. Stream function

Boundary (a), (b), (f) and (d) shown in Fig. 1

$$\overline{\varphi}=0$$

2.2.3. Temperature

Boundary (e) shown in Fig. 1

$$T^*=1.0$$

Boundary (a) and (b)

$$T^*=0.0$$

Boundary (c) and (d)

$$\frac{\partial T^*}{\partial n}=0.0$$

Boundary (f), the interface of fluid region and solid region

$$T_{\mathrm{f}}^*=T_{\mathrm{s}}^*$$

$$k_{\mathrm{f}}\left(\frac{\partial T^*}{\partial Y}\right)_{\mathrm{f}}=k_{\mathrm{s}}\left(\frac{\partial T^*}{\partial Y}\right)_{\mathrm{s}}$$

$$\left(\frac{\partial T^*}{\partial Y}\right)_{\mathrm{f}}=k\left(\frac{\partial T^*}{\partial Y}\right)_{\mathrm{s}}$$

2.2.4. Settings for solid region

$$v=10^{20}$$

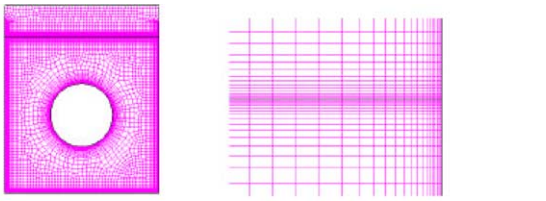

Fig. 2. Grid distribution scheme.

2.3. Grids and conjugate details

Because of the complex geometric shape we use non-structured grid system (Fig. 2). The grid is dense near the boundary and loose deep into the internal due to the sensitivity of the result to the boundary. Especially on the interface we choose symmetric grid distribution on both sides of this interface. The closer to this interface, the denser the grid is.

In order to get the temperature on the interface, we extend the temperatures on both sides in Taylor series

$$T^*_{\mathrm{ns}} = T^* + \frac{\partial T^*}{\partial Y} \times \delta Y + \frac{(\delta Y)^2}{2!} \frac{\partial^2 T^*}{\partial Y^2}$$

$$T^*_{\mathrm{nf}} = T^* + \frac{\partial T^*}{\partial Y} \times (-\delta Y) + \frac{(-\delta Y)^2}{2!} \frac{\partial^2 T^*}{\partial Y^2}$$

We delete the δY term by combine the two extensions. Considering the interface temperature boundary condition

$$\left(\frac{\partial T^*}{\partial Y}\right)_{\mathrm{f}} = k\left(\frac{\partial T^*}{\partial Y}\right)_{\mathrm{s}}$$

We can deduce the temperature on the interface as Eq. (9)

$$T^* = \frac{kT^*_{\mathrm{ns}} + T^*_{\mathrm{nf}}}{(1+k)} + \mathrm{O}(\delta Y^2) \tag{9}$$

In our dimensionless calculation field, δY is selected as 0.0005, So when we use equation (9) the error brought by difference is $(0.0005)^2$. This is slight enough to be accepted in simulation.

3. Results and discussion

In order to test our whole simulation scheme, we simulated the flow in porous media described in [10]. By using the completely same parameters of $Ra = 10^3$ we got very accurate results. This demonstrates that by combining symmetric grid on both side of boundary (f) and formula (9) to conjugate convection and conduction is feasible.

In order to evaluate the overall heat transfer rate in this research, we defined local Nusselt number Nu and overall mean Nusselt number Nu_{mean}, referred to high temperature horizontal cylinder.

$$Nu = \left|\frac{\partial T^*}{\partial X}\right| \times \frac{2|X - X_{\mathrm{c}}|}{B} + \left|\frac{\partial T^*}{\partial Y}\right| \times \frac{2|Y - Y_{\mathrm{c}}|}{B} \tag{10}$$

$$Nu_{\mathrm{mean}} = \frac{1}{\pi B} \oint Nu \, \mathrm{d}s \tag{11}$$

3.1. Stream lines and temperature distributions

First we present distributions of stream and temperature in the calculated domain of different conductivity ratios on the condition of $Ra = 10^4$, $A = 1.0$, $B = 0.4$, $C = 0.2$ (shown in Fig. 3). From Fig. 3 we can find both stream function and temperature distributions vary with k, especially the temperature distributions are different from each other clearly. The figures of c^* series here are the dimensionless temperatures of three concerned boundaries, they are lower adiabatic boundary symbolized by (d) in Fig. 1, interface of solid region and flow field labeled by (f), the upper adiabatic boundary annotated by (c) in Fig. 1, respectively. From c^* series we can find that the temperature distributions change greatly with conductivity ratio k. When k is less than 1, the temperature of the interface is greater than that of upper boundary at any X position, both of them are greater than the temperature of the lower boundary at the same X position. On the contrary, when k is greater than 1, the temperature of interface is less than that of the lower adiabatic boundary at any X position. Just as we expected, the temperature of interface is always greater than that of the upper horizontal adiabatic boundary at any X position in spite of k.

3.2. Influence of material characteristics and dynamic parameter on Nu_{mean}

In order to analyze the influence of material characteristics and dynamic parameter on the overall heat transfer rate. We fixed geometrical shape of our calculated domain and vary conductivity ratio k. The fixed condition we chose here is $A = 1$, $B = 0.4$, $C = 0.2$. From Fig. 4, it can be concluded that the overall Nu number increases with the increase of k and Ra.

3.3. Influence of geometric shape on the overall heat transfer rate

This time dynamic parameter is fixed at $Ra = 10^4$. Under this condition, we analyzed the influence of some geometric parameters on the overall heat transfer rate at three typical k values. From Figs. 5–7 we can find they

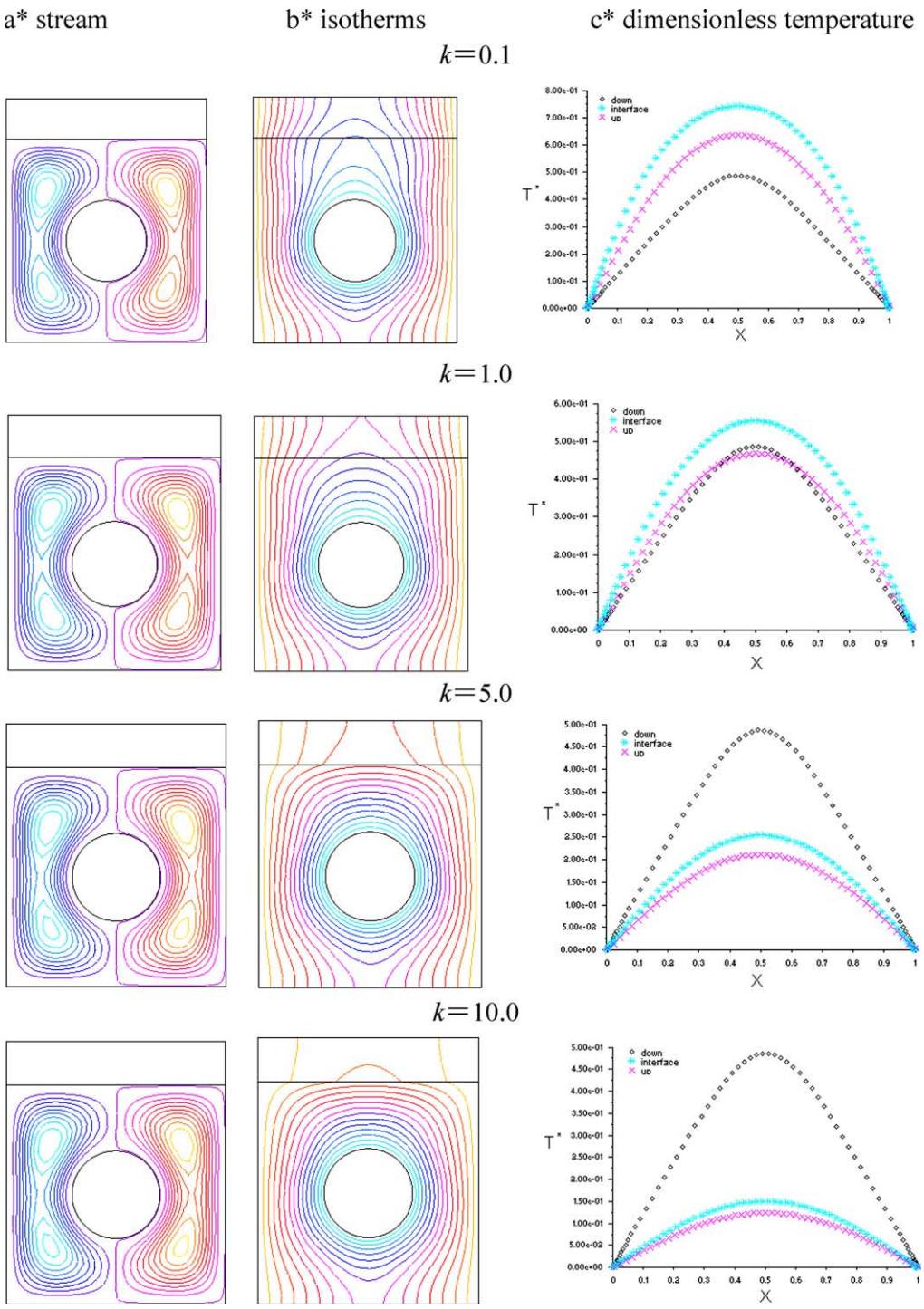

Fig. 3. Calculated stream and temperature distributions.

have one point in common, that is the overall heat transfer rate increase with the increase of k. This trend is compared well with the trend in Fig. 4.

Fig. 5 presents the variation of Nu_{mean} with the change of A, the ratio of cavity height to its width. From it we can find Nu_{mean} increases with the increase of A. But

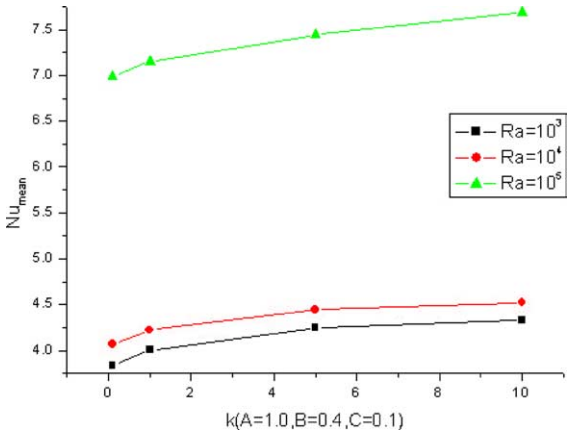

Fig. 4. Variation of overall mean Nu with k at different Ra.

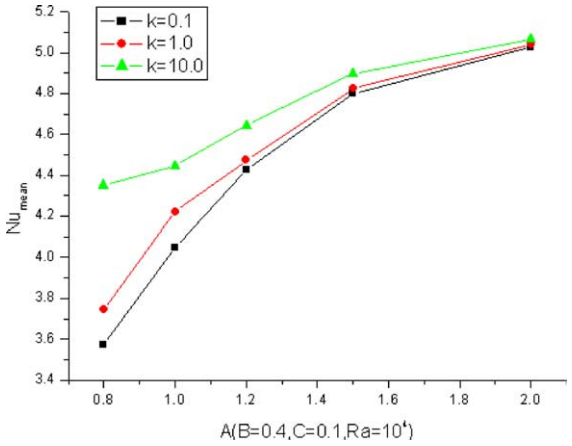

Fig. 5. Variation of Nu_{mean} with the variation of A at different k.

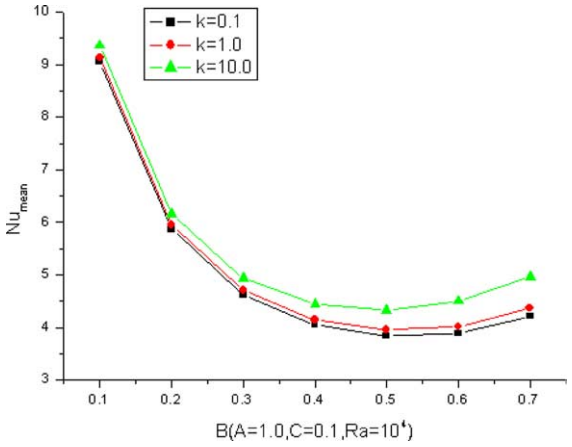

Fig. 6. Variation of Nu_{mean} with the variation of B at different k.

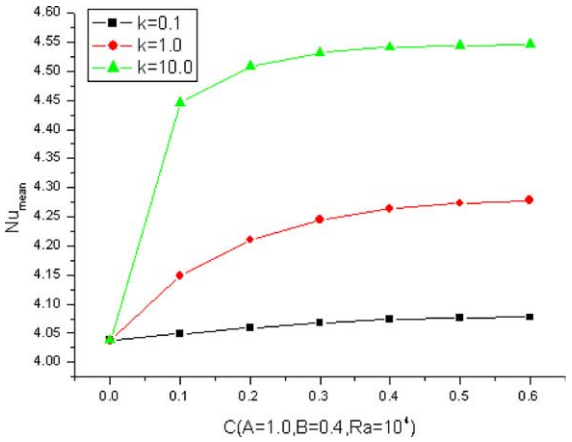

Fig. 7. Variation of Nu_{mean} with the variation of C at different k.

as A increasing the change of Nu_{mean} due to the variation of k is much slighter. Especially when A is larger than 1.5 the overall heat transfer is not sensitive to the solid material conductivity any more.

Fig. 6 gives the variation of Nu_{mean} with the variation of B, the relative diameter of hot temperature horizontal cylinder. Since variation of B is confined to $(0,1)$, our research range is from 0.1 to 0.7. During this range it can be seen that the overall heat transfer rate first decreases with the increase of relative diameter and then reaches its minimum at about $B = 0.5$ and thereafter increases with B. At the same time the change of Nu_{mean} due to variation of k is more and more clear as B increases.

Fig. 7 shows the influence of the relative solid region thickness C on the overall heat transfer rate. The whole trend is that Nu_{mean} increases with the increase of C under all the three typical k. It is notable that when value C is very small Nu_{mean} increases faster with C, but when C is large enough Nu_{mean} increases slightly with C. This demonstrates Nu_{mean} changes less and less as C increases.

4. Conclusions

1. Our scheme of combining symmetric grid system on both sides of conjugate interface (f) and Eq. (9) to simulate fluid with solid region is successful. This is very useful to simulate other similar problems.
2. Overall heat transfer rate represented by number Nu_{mean} increases with k and dynamic parameter Ra.
3. The geometric parameters affect Nu_{mean} greatly. According to Fig. 5, when A is large enough Nu_{mean} changes little with the increase of k, This is because the cold wall is relatively long and the convection dominates the overall heat transfer. On the other hand the conduction in solid is unimportant in spite of the thermal properties of the solid region. Figs. 6 and 7 present a similar phenomena. In Fig. 6 when

B becomes large enough Nu_{mean} changes greatly with the thermal properties. This is because the solid region is relatively near the hot wall and the conduction in the solid region dominates, hence the Nu_{mean} is sensitive to the thermal properties. Fig. 7 tells us k is the major factor. This point can be assimilated to the thermal resistance. There exists a relatively dominant factor and we should pay special attention to the important factors.

References

[1] M. Hortmann, M. Peric, Volume multi-grid prediction of laminar natural convection: bench-mark solutions, Int. J. Numer. Methods Fluids 11 (1990) 189–207.

[2] G. Barakos, E. Mitsoulis, Natural convection flow in a square cavity revised laminar and turbulent models with wall function, Int. J. Numer. Methods Fluids 18 (1994) 695–719.

[3] Q.-H. Deng, G.-F. Tang, Y. Li, A combined temperature scale for analyzing natural convection in rectangular enclosures with discrete wall heat sources, Int. J. Heat Mass Transfer 45 (2002) 3437–3446.

[4] G. Jilani, S. Jayaraj, K. Khadarvoli, Numeric analysis of free convective flows in partially open enclosure, Heat Mass Transfer 38 (2002) 267–270.

[5] W. Gao, W. Lin, E. Lu, numerical study on natural convection inside the channel between the flat-plate cover and sine-wave absorber of a cross-corrugated solar air heater, Energy Conver. Manage. 41 (2000) 145–151.

[6] J.P. Liu, W.Q. Tao, Numerical analysis of natural convection around a vertical channel in a rectangular enclosure, Heat Mass Transfer (1996) 313–321.

[7] G. Cesini, M. Paroncini, G. Cortella, M. Manzan, Natural convection from a horizontal cylinder in a rectangular cavity, Int. J. Heat Mass Transfer 24 (1999) 1801–1811.

[8] M. Lacroix, A. Joyeux, Coupling of wall conduction with natural convection from heated cylinders in a rectangular enclosure, Int. Commun. Heat Mass Transfer 23 (1) (1996) 143–151.

[9] W.Q. Tao, Numerical Heat Transfer, second ed., Xian, China, pp. 310–311.

[10] A.C. Baytas, A. Liaqat, I. Pop, Conjugate natural convection in a square porous cavity, Heat Mass Transfer 37 (2001) 467.